

## Electrochemical performance of $\text{LiFePO}_4\text{-Li}_3\text{V}_2(\text{PO}_4)_3$ composite material prepared by solid-hydrothermal method

GUO Xiao-dong<sup>1</sup>, ZHONG Ben-he<sup>1</sup>, LIU Heng<sup>2</sup>, SONG Yang<sup>1</sup>, WEN Jia-jie<sup>1</sup>, TANG Yan<sup>1</sup>

1. School of Chemical Engineering, Sichuan University, Chengdu 610065, China;

2. School of Materials Science and Engineering, Sichuan University, Chengdu 610065, China

Received 26 August 2010; accepted 26 April 2011

**Abstract:**  $\text{LiFePO}_4\text{-Li}_3\text{V}_2(\text{PO}_4)_3$  composites were synthesized by solid-hydrothermal method and by ball milling, respectively. The electrochemical performance of the solid-hydrothermally obtained materials (C-LFVP) was significantly improved compared with  $\text{LiFePO}_4$  (LFP) and  $\text{Li}_3\text{V}_2(\text{PO}_4)_3$  (LVP), and it was also much better than that of the ball-milled  $\text{LiFePO}_4\text{-Li}_3\text{V}_2(\text{PO}_4)_3$  (P-LFVP). C-LFVP and P-LFVP both had four REDOX peaks (voltage plateaus), which coincided with that of LFP and LVP. Some new trace substances were found in C-LFVP which had more perfect morphology, this was responsible for the better electrochemical performance of C-LFVP than P-LFVP.

**Key words:**  $\text{LiFePO}_4$ ;  $\text{Li}_3\text{V}_2(\text{PO}_4)_3$ ; composite materials; solid-hydrothermal

### 1 Introduction

In recent years, environmental pollution and energy crisis make it high time to develop green vehicles. A reliable and highly-functional battery is essential to guarantee a successful development. The lithium-ion battery has attracted increasing attention for its consistent performance. Cathode is the key element of the lithium-ion battery, and lithium metal oxides are known as the most popular materials for the lithium-ion battery cathode [1–3]. However, the low thermal stability of lithium metal oxides hinders its large-scale application in electric vehicles. In contrast, poly-anionic phosphate materials such as lithium iron phosphate ( $\text{LiFePO}_4$ ) and lithium vanadium phosphate ( $\text{Li}_3\text{V}_2(\text{PO}_4)_3$ ) exhibit good thermal stability and high voltage, which makes them the most promising cathode candidates so far. However,  $\text{LiFePO}_4$  and  $\text{Li}_3\text{V}_2(\text{PO}_4)_3$  have their own advantages and drawbacks.  $\text{LiFePO}_4$  has a stable voltage platform and its cyclic attenuation rate is almost negligible, but its relatively low capacity and low voltage limit its energy density and consequently limits its use. Although  $\text{Li}_3\text{V}_2(\text{PO}_4)_3$  has a higher voltage, it invariably suffers from its stepped voltage platforms and severe cycle

attenuation [4–6]. In order to integrate the technical advantages from different materials, scientists have proposed the use of hybrid materials. As all known metal doping can improve the performance of cathode material [7], YANG et al [8] improved performance of  $\text{LiFePO}_4$  by adding vanadium. However, doping can only improve the main material, and cannot integrate the advantages of two active materials.

ZHENG et al [9] reported that  $\text{LiFePO}_4\text{-LiMn}_2\text{O}_4$  hybrid materials had excellent performance by mixing well-prepared  $\text{LiFePO}_4$  and  $\text{LiMn}_2\text{O}_4$ , which was called physical-mixing method. WU et al [10] also did series research on the effect of  $\text{LiMn}_2\text{O}_4/\text{LiCoO}_2$  blender positive material of Li-ion batteries, the experimental results showed that the cycle performance of Li-ion battery used  $\text{LiMn}_2\text{O}_4$  blended  $\text{LiCoO}_2$  was good at ambient and high temperature. So it is easy to think blind  $\text{LiFePO}_4$  and  $\text{Li}_3\text{V}_2(\text{PO}_4)_3$ . WANG et al [11] added  $\text{Li}_3\text{V}_2(\text{PO}_4)_3$  in  $\text{LiFePO}_4$  and found that the blending material had combined performance of the two materials. XIANG et al [12] reported that  $9\text{LiFePO}_4\text{-Li}_3\text{V}_2(\text{PO}_4)_3/\text{C}$  synthesized by simple solid-state method exhibited reversible discharge capacities both at 0.1 C and 10 C, it was stressed that the most important reason was that there were two phases of V-doped LFP and Fe-doped

LVP in hybrid materials. ZHENG et al [13–16] achieved much progress in hybrid materials, such as different proportion of  $\text{LiFePO}_4$  and  $\text{Li}_3\text{V}_2(\text{PO}_4)_3$  on the performance of the materials and the reaction mechanism. The synthesized composite materials exhibited better electrochemical performance than individual  $\text{LiFePO}_4$  and  $\text{Li}_3\text{V}_2(\text{PO}_4)_3$ , which indicated that  $\text{LiFePO}_4$  and  $\text{Li}_3\text{V}_2(\text{PO}_4)_3$  can be sufficiently compatible to create an effective hybrid material. However, most hybrid materials synthesized by usual solid method have many disadvantages, so the performance of the materials was improved less than expected.

In this work,  $\text{LiFePO}_4\text{-Li}_3\text{V}_2(\text{PO}_4)_3$  hybrid material was prepared by a novel method called solid-hydrothermal method and usual solid method in order to explain different effect of preparation on the electrochemical performance.

## 2 Experimental

### 2.1 Preparation

#### 2.1.1 Solid-hydrothermal method

Stoichiometric  $\text{LiH}_2\text{PO}_4$  (99.9%),  $\text{FeC}_2\text{O}_4\cdot 2\text{H}_2\text{O}$  (99.95%) and  $\text{V}_2\text{O}_5$  (99%) were employed as starting materials, they were ball milled for 10 h to get powder mixtures, the mixtures were added in a certain amount deionized water and then put in an autoclave for hydrothermal reaction at 180 °C. After 8 h, the reaction stopped and the solution was then filtered to get filter cake, the filter cake was mixed with glucose to get a precursor. The precursor was calcined at 600 °C for 4 h in nitrogen to get C-LFVP samples.

#### 2.1.2 Comparative experimental method

Stoichiometric  $\text{LiH}_2\text{PO}_4$  and  $\text{FeC}_2\text{O}_4\cdot 2\text{H}_2\text{O}$  with glucose were ball milled for 10 h to obtain a precursor, then the precursor was heated at 800 °C under nitrogen for 20 h to get LFP.  $\text{FeC}_2\text{O}_4\cdot 2\text{H}_2\text{O}$  was replaced with  $\text{V}_2\text{O}_5$ . The same method and other ingredients were used to obtain LVP. The LFP and LVP were mixed by ball milling for 2 h to get P-LFVP.

### 2.2 Characterization

X-ray diffraction (D/max-rB, Rigaku,  $\text{Cu K}_\alpha$  radiation) was used to analyze the crystalline structure of the samples with software Jade 5.0. The microstructures of the samples were obtained by a SPA400 Seiko Instruments scanning electron microscope (SEM). The conductivity was measured in a D41-11C/ZM four-probe resistivity tester. An EA3000 elemental analyzer and a Shimadzu AXIS-ULTRA DLD photoelectron spectroscopy were utilized to determine the carbon content. CV curves were obtained with Princeton Applied Research PARSTAT2273 electrochemical workstations.

The electrochemical properties of samples were evaluated with coin-type CR2032 cells. The cathode film was prepared with active material, acetylene black and polyvinylidene fluoride (PVDF) binder at a mass ratio of 80:15:5. A metallic lithium film was used as the anode, the electrolyte was prepared with 1 mol/L  $\text{LiPF}_6$  dissolved in a mixture of ethylene carbonate (EC), propylene carbonate (PC) and diethyl carbonate (DEC) with volume ratio of 1:1:1, and a Celgard 2400 micro-porous membrane was used as the separator. The cell was assembled in a glove box with protective gas of pure argon. The cell was tested galvanostatically with a multichannel battery test system (Neware BTS-610, Shenzhen, China) at room temperature.

## 3 Results and discussion

Charge/discharge cycle performance of the samples was measured at 0.1 C in the voltage range of 2.5–4.3 V, 2.5–4.8 V and 3.0–4.8 V. Figure 1 shows the specific discharge capacities of the samples and the initial specific discharge capacity and attenuation after 15 cycles are listed in Table 1. It is noted that the C-LFVP exhibits much better electrochemical performance, higher discharge capacity and lower attenuation than P-LFVP.

The C-LFVP discharge capacities are about 168, 190, and 160 mA·h/g in the voltage range of 2.5–4.3 V, 2.5–4.8 V and 3.0–4.8 V, respectively. Compared with LFP, the discharge capacities of which are about 156 and 162 mA·h/g in the voltage range of 2.5–4.3 V and 2.5–4.8 V, respectively, it is obvious that in the high voltage range, the capacity of the C-LFVP is much higher than that of the LFP, which shows that the LVP plays a key role in the high voltage range. Compared with the LVP, the discharge capacities of which are about 153 and 169 mA·h/g in the voltage range of 3.0–4.5 V and 2.5–4.8 V, respectively. There are two advantages of the higher capacity and the better cycle stability. The theoretical capacity of the LVP is 199 mA·h/g, but in the charge/discharge process, only part of Li in the LVP is electrochemically active, which limits the actual capacity far below 199 mA·h/g and makes the capacity fades with cycling. In the C-LFVP, the two weaknesses of the LVP are overcome. On the other hand, improvements are not found in the P-LFVP.

Figure 2 shows the charge/discharge voltage plateaus of the samples at 0.1 C. The plateaus of P-LFVP are similar to those of the C-LFVP. Between 3.5 and 4.0 V, there are faintly two plateaus on the charge curves of the P-LFVP and C-LFVP, which corresponds to those of the LFP and LVP. The other two plateaus at 4.0 and 4.3 V on the charge curves of the P-LFVP and C-LFVP coincide with those of the LVP. The discharge curves of

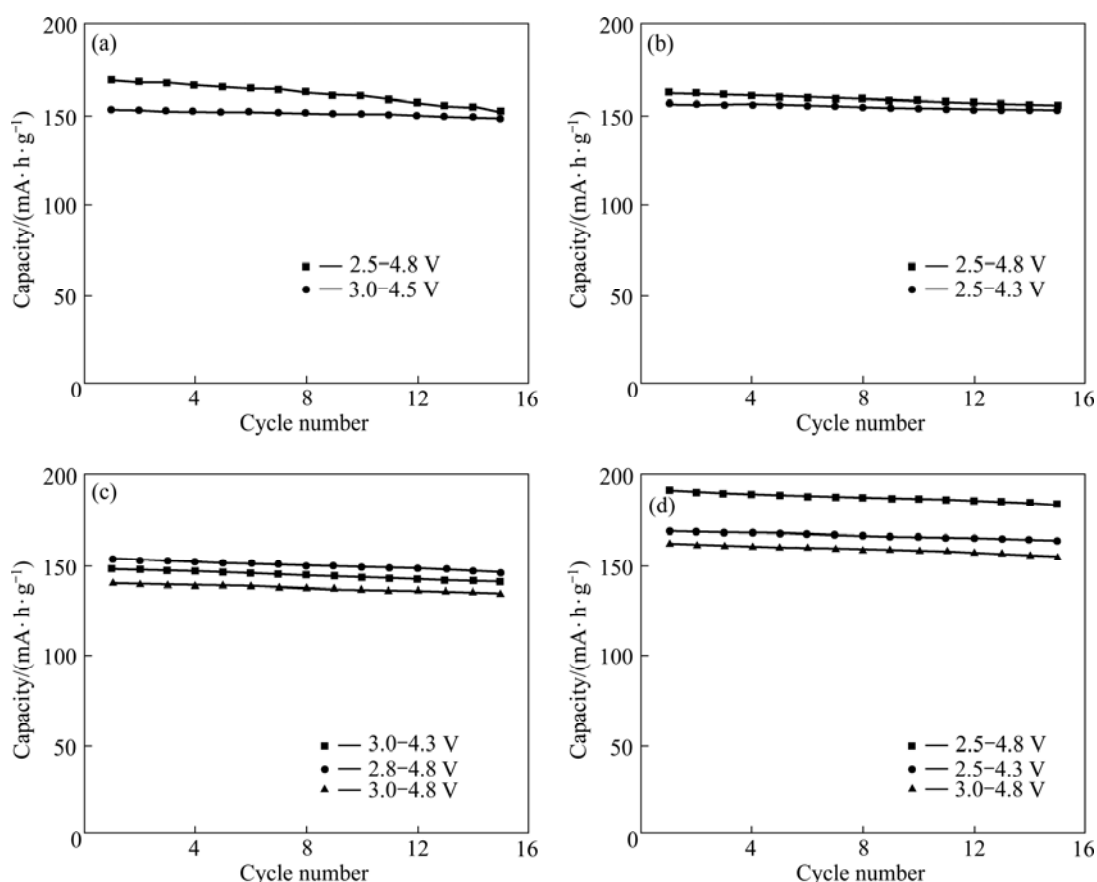


Fig. 1 Discharge capacity of LVP (a), LFP (b), P-LFVP (c) and C-LFVP (d) at 0.1 C in different voltage ranges

Table 1 Specific capacity and retention of samples after 15 cycles at 0.1 C

Alloy	Voltage range/V	Initial capacity/ (mA·h·g <sup>-1</sup> )	Retention/%
LVP	2.5–4.3	–	–
	2.5–4.8	169.88	94.8
	3.0–4.5/4.8	153.15	97.3
LFP	2.5–4.3	156.56	97.5
	2.5–4.8	162.89	95.2
	3.0–4.5/4.8	–	–
P-LFVP	2.5–4.3	148.23	95.3
	2.5–4.8	153.89	95.0
	3.0–4.5/4.8	140.12	96.0
C-LFVP	2.5–4.3	168.56	97.0
	2.5–4.8	191.56	95.8
	3.0–4.5/4.8	161.55	95.6

the P-LFVP and C-LFVP are also similar to those of the LFP and LVP. The CV curves of the C-LFVP are consistent with those of the P-LFVP; the four REDOX peaks at 4.13/3.99 V, 3.72/3.62 V, 3.63/3.54 V and 3.53/3.35 V (see Fig. 3(a)) match those of the LFP (3.55/3.34 V) and LVP (4.12/4.0 V, 3.71/3.62 V,

3.63/3.54 V), as shown in Fig. 3(b). All these data indicate that in the LiFePO<sub>4</sub>-Li<sub>3</sub>V<sub>2</sub>(PO<sub>4</sub>)<sub>3</sub> (including the P-LFVP and C-LFVP) composites, the LFP and LVP act independently.

Figure 4 shows the X-ray diffraction patterns of the LFP, LVP, P-LFVP and C-LFVP. It could be inferred that C-LFVP has a nice crystalline structure from its smooth base lines, sharp peak lines and the main peaks of the C-LFVP overlap with the main peaks of LFP and LVP. However, there are many weak impurity phases matching the trace of LiFeO<sub>2</sub>, Fe<sub>2</sub>P and Li<sub>2</sub>O, all of which can be contributed to Li-ion transportation. In comparison, with its uneven base lines, moderate peak lines and mediocre intensity, the X-ray diffraction pattern of P-LFVP suggests that its crystalline structure is far from satisfactory. For P-LFVP, enormous thermal energy is consumed to reshape the crystalline structure of the material during the ball milling process. All above explain the excellent electrochemical performance of the C-LFVP. Table 2 shows the crystalline lattice parameters and crystallites of the samples obtained from Rietveld refinement by Jade 5.0 Crystal Data Processing software. The cell volume of the C-LFVP is nearly the summation of that of the LFP and the LVP, which indicates that the LFP molecule and LVP molecule share chemical

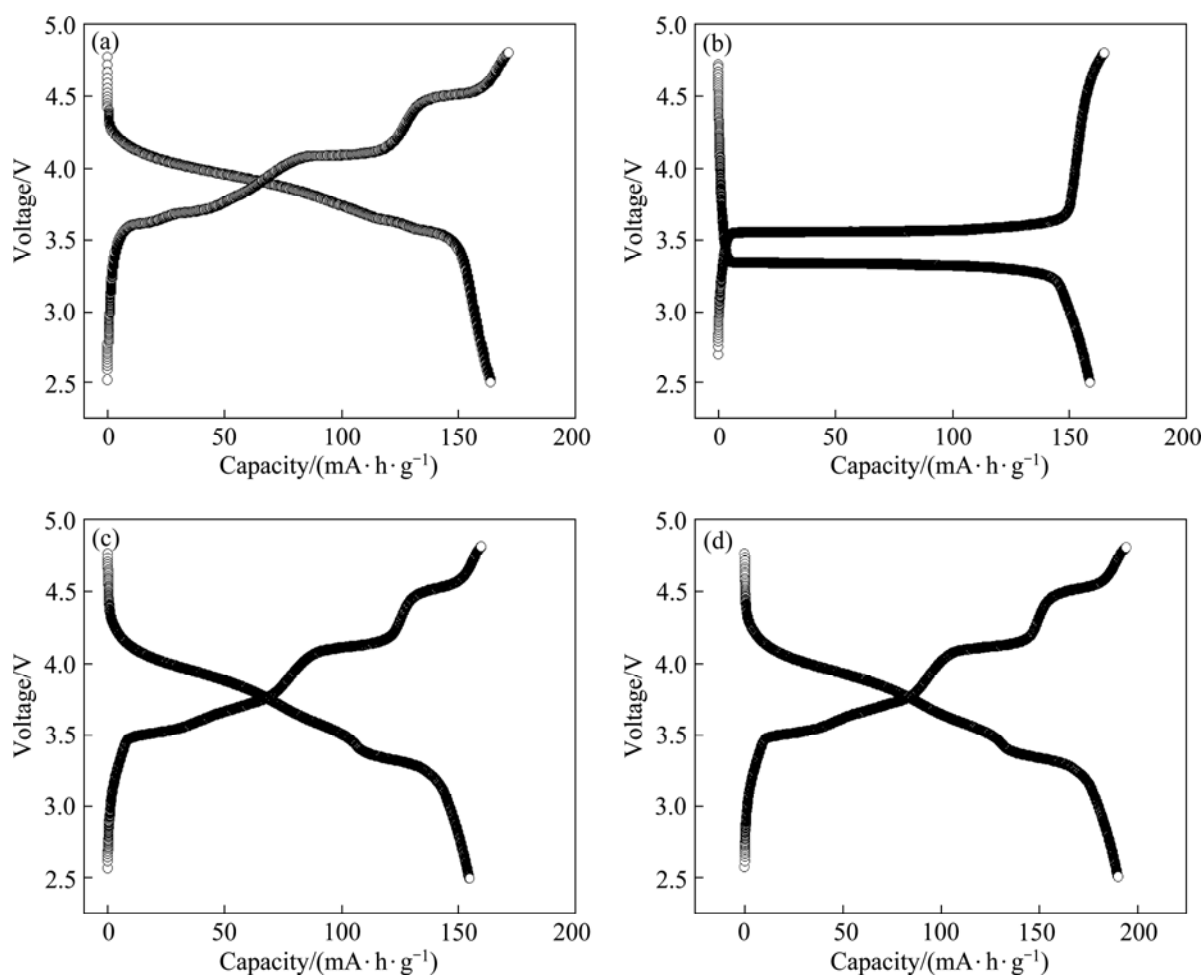


Fig. 2 Voltage plateaus of samples at 0.1 C in voltage range of 2.5–4.8 V: (a) LVP; (b) LFP; (c) P-LFVP; (d) C-LFVP

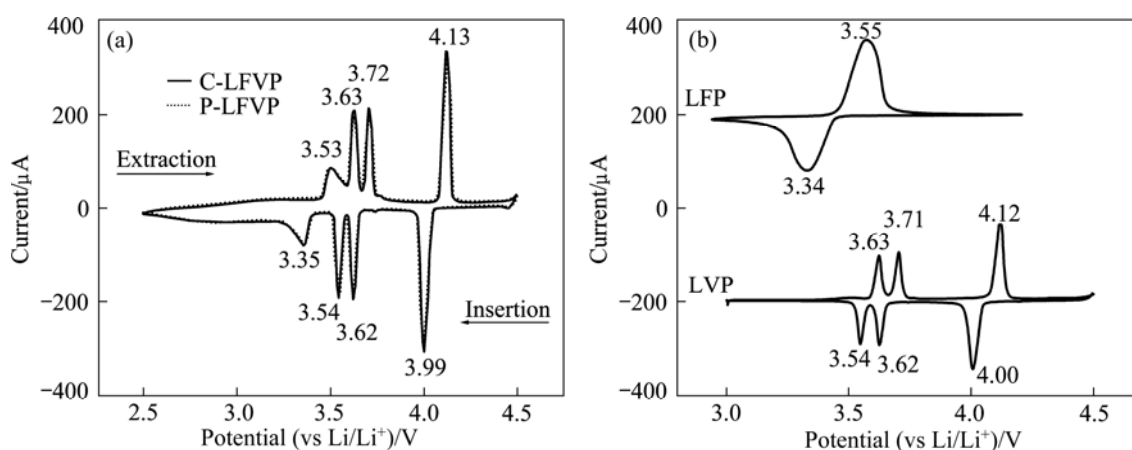


Fig. 3 Cyclic voltammograms of P-LFVP, C-LFVP(a) and LFP, LVP (b)

bonds in the C-LFVP molecule while keep their own crystal structure, so they make good performance without interfering with each other. Small crystallite of C-LFVP is another guarantee for excellent electrochemical performance.

Figure 5 shows the SEM images of the samples. It is clear that C-LFVP has the minimum grain size of

about 400 nm, the most regular morphology and the smoothest surface among the samples, which is due to the preparation method. In the solid-hydrothermal method process, the starting materials are fully blended by ball milling and then transferred to a homogeneous high-temperature and high-pressure liquid state environment to react. The ball-milling step fully

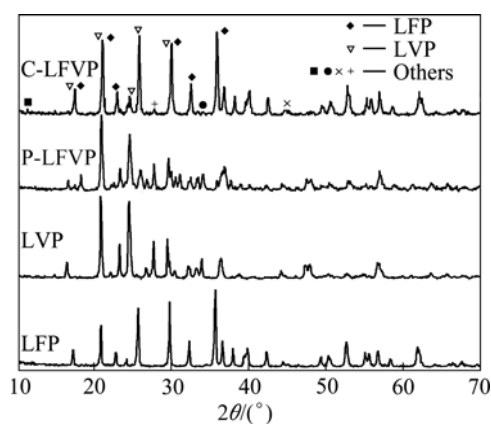


Fig. 4 XRD patterns of LFP, LVP, P-LFVP and C-LFVP

Table 2 Lattice parameters, unit cell volumes and crystallites of samples

Alloy	a/ nm	b/ nm	c/ nm	Angle/ (°)	V/ nm <sup>3</sup>	Crystallite/ Å
LFP	1.032 2	0.598 2	0.465 8	90.00	0.287 7	450
LVP	0.401 6	1.204 7	0.632 2	108.27	0.290 4	350
P-LFVP	0.705 2	0.923 4	0.643 1	90.00	0.418 7	550
C-LFVP	0.819 3	0.769 8	0.635 8	90.00	0.401	350

guarantees the uniformity of the product, and liquid medium can effectively prevent the grains growing up in the next step. In the opposite, intense mechanical ball milling damages the surface structure, especially the carbon-coated layer on the top of P-LFVP. Compared with its predecessors LFP and LVP (samples before ball

milling), P-LFVP has a very rough surface, and tiny carbon particles are scattered around the P-LFVP grains. The XPS spectra of P-LFVP and C-LFVP are shown in Fig. 6. It is seen that the carbon content on the surface of C-LFVP grain is much higher than that of P-LFVP grain, which indicates carbon combines firmly on the surface of the C-LFVP grain. As a result, although the P-LFVP material has the same total carbon content as C-LFVP, the carbon content in grain surface is less than that in the C-LFVP. Consequently, the conductivity of P-LFVP is orders lower than that of C-LFVP, as listed in Table 3, which was explained in detail in Ref. [17].

Table 3 Carbon content and conductivity of samples

Alloy	Carbon content/%	Conductivity/(S·cm <sup>-1</sup> )
P-LFVP	4.5	2.3×10 <sup>-4</sup>
C-LFVP	4.2	3.5×10 <sup>-2</sup>

### 4 Conclusions

1) LiFePO<sub>4</sub>-Li<sub>3</sub>V<sub>2</sub>(PO<sub>4</sub>)<sub>3</sub> hybrid materials for the Lithium-ion battery were prepared by solid-hydrothermal method and ball milling for comparison. LFP and the LVP are independent on the C-LFVP, but their chemical bonds overlap partially.

2) XRD patterns show trace impurities. SEM images show the C-LFVP had smaller size, more regular morphology and a more complete carbon layer on the grain surface than the P-LFVP, which account for better conductivity of the C-LFVP, although the two samples have a similar total carbon content.

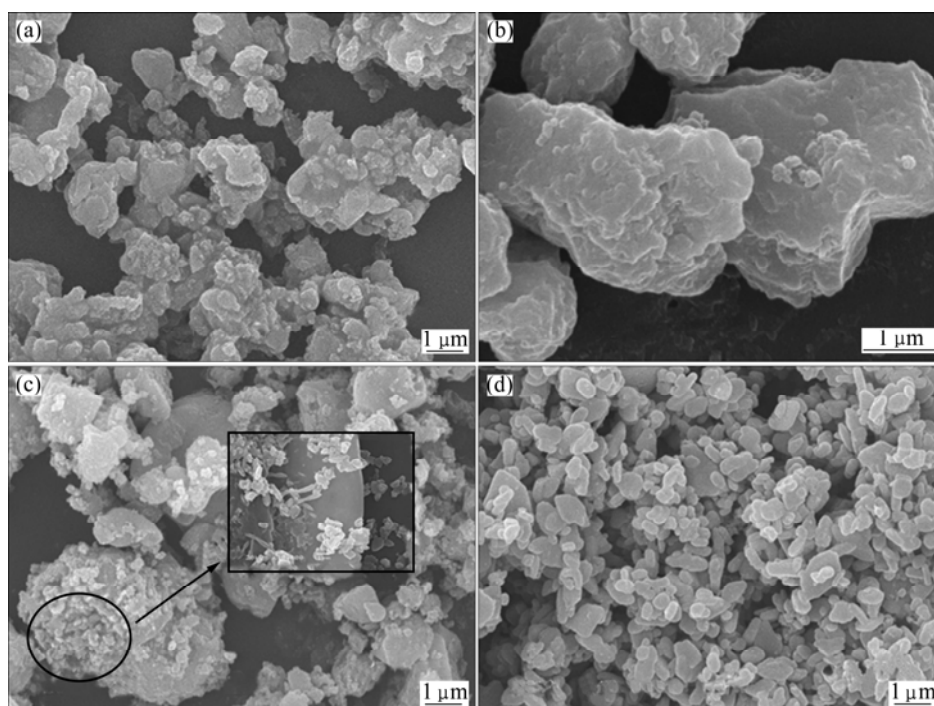


Fig. 5 SEM images of LVP (a), LFP (b), P-LFVP (c) and C-LFVP (d)

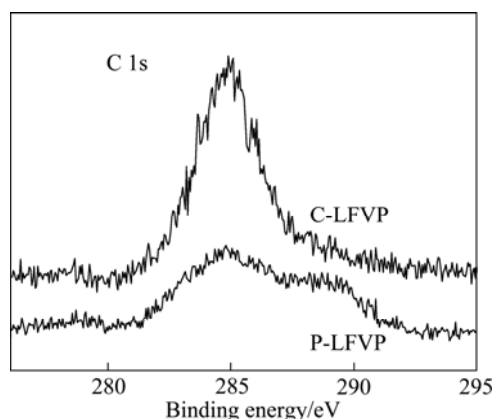


Fig. 6 XPS spectra of P-LFVP and C-LFVP

3) At 0.1C, the C-LFVP cathode material has a discharge capacity of 190 mA·h/g, far more than that of the P-LFVP. So a solid-hydrothermal reaction is a preferred method to prepare  $\text{LiFePO}_4\text{-Li}_3\text{V}_2(\text{PO}_4)_3$  hybrid material.

## References

- [1] FERGUS J W. Recent developments in cathode materials for lithium ion batteries [J]. *J Power Sources*, 2010, 195(4): 939–954.
- [2] YANG Zhi, LI Xin-hai, WANG Zhi-xing, PENG Wen-jie, GUO Hua-jun. Synthesis and characterization of high tap-density spherical  $\text{LiNi}_{0.5}\text{Co}_{0.2}\text{Mn}_{0.3}\text{O}_2$  powders [J]. *The Chinese Journal of Nonferrous Metals*, 2010, 20(1): 106–111. (in Chinese)
- [3] ZHAO Ming-shu, WANG Fei, SONG Xiao-ping. Synthesizing kinetics and characteristics of  $\text{LiMnCoO}_4$  using as lithium-ion battery cathode material [J]. *The Chinese Journal of Nonferrous Metals*, 2005, 15(9): 1396–1342. (in Chinese)
- [4] MANICKAM M, TAKATA M. Effect of cathode binder on capacity retention and cycle life in transition metal phosphate of a rechargeable lithium battery [J]. *Electrochimica Acta*, 2003: 48: 957–963.
- [5] HUANG H, FAULKNER T, BARKER J, SAIDI M Y. Lithium metal phosphates, power and automotive applications [J]. *J Power Sources*, 2009, 189(1): 748–751.
- [6] ZHONG Mei-e, ZHOU Zhi-hui, ZHOU Zhen-tao. Effects of  $\text{Fe}^{3+}$  sources on structure and properties of  $\text{LiFePO}_4/\text{C}$  prepared by carbonthermal reduction method [J]. *The Chinese Journal of Nonferrous Metals*, 2009, 19(8): 1462–1467. (in Chinese)
- [7] RUAN Yan-li, TANG Zhi-yuan. Effects of  $\text{Mg}^{2+}$  doping on structure and electrochemical performance of  $\text{LiFePO}_4$  [J]. *The Chinese Journal of Nonferrous Metals*, 2005, 15(9): 1416–1420. (in Chinese)
- [8] YANG Mu-Rong, KE Wei-hsin, WU She-huang. Improving electrochemical properties of lithium iron phosphate by addition of vanadium [J]. *Journal of Power Sources*, 2007, 165(2): 646–650.
- [9] ZHNEG Li-juan, LU Xing-he, CUI Yan. The performance of Li-ion battery using  $\text{LiFePO}_4\text{-LiMn}_2\text{O}_4$  mixed cathode [J]. *Battery Bimonthly* 2010; 40(1): 33–35. (in Chinese)
- [10] WU Xue-feng, WANG Zhen-bo, ZHANG Ming-yan. Effect of  $\text{LiMn}_2\text{O}_4/\text{LiCoO}_2$  blender positive material on the performance of Li-ion batteries [J]. *Chinese Battery Industry*, 2010, 15(2): 98–102.
- [11] WANG Li-na, LI Zheng-chun, XU Hong-jie, ZHANG Ke-li. Studies of  $\text{Li}_3\text{V}_2(\text{PO}_4)_3$  additives for the  $\text{LiFePO}_4$ -based Li ion batteries [J]. *J Phys Chem C*, 2008, 112(1): 308–312.
- [12] XIANG Jia-yuan, TU Jiang-ping, ZHANG Li, WANG Xiao-li, ZHOU Yi, QIAO Yong-qin, LU Yun. Improved electrochemical performances of  $9\text{LiFePO}_4\text{-Li}_3\text{V}_2(\text{PO}_4)_3$  composite prepared by a simple solid-state method [J]. *J Power Sources*, 2010, 195(24): 8331–8335.
- [13] ZHENG Jun-chao, LI Xin-hai, WANG Zhi-xing, LI Jin-hui, LI Ling-jun, WU Ling, GUO Hua-jun. Characteristics of  $x\text{LiFePO}_4\cdot y\text{Li}_3\text{V}_2(\text{PO}_4)_3$  electrodes for lithium batteries [J]. *Ionics*, 2009, 15(6): 753–759.
- [14] ZHENG Jun-chao, LI Xin-hai, WANG Zhi-xing, QIN Dong-mian, GUO Hua-jun, PENG Wen-jie. Synthesis and characterization of composite cathode material  $x\text{LiFePO}_4\cdot y\text{Li}_3\text{V}_2(\text{PO}_4)_3$  [J]. *Journal of Inorganic Materials*, 2009, 24(1): 143–146.
- [15] ZHENG Jun-chao, LI Xin-hai, WANG Zhi-xing, LI Jin-hui, WU Ling, LI Ling-jun, GUO Hua-jun. A coalescence mechanism for the composite cathode material  $x\text{LiFePO}_4\cdot y\text{Li}_3\text{V}_2(\text{PO}_4)_3$  [J]. *Acta Physchim Sin*, 2009, 25(9): 1916–1920.
- [16] ZHENG Jun-chao, LI Xin-hai, WANG Zhi-xing, LIU Sha-sha, LIU De-rong, WU Ling, LI Ling-jun, LI Jing-hui, GUO Hua-jun. Novel synthesis of  $\text{LiFePO}_4\text{-Li}_3\text{V}_2(\text{PO}_4)_3$  composite cathode material by aqueous precipitation and lithiation [J]. *J Power Sources*, 2010, 195(9): 2935–2938.
- [17] GUO Xiao-dong, ZHONG Ben-he, LIU Heng, TANG Yan, WU De-qiao. The preparation of  $\text{LiFePO}_4/\text{C}$  cathode by a modified carbon-coated method [J]. *J Electrochem Soc A*, 2009, 156(10): 787–790.

# 固相-水热法制备 $\text{LiFePO}_4\text{-Li}_3\text{V}_2(\text{PO}_4)_3$ 复合材料及其电化学性能

郭孝东<sup>1</sup>, 钟本和<sup>1</sup>, 刘恒<sup>2</sup>, 宋杨<sup>1</sup>, 文嘉杰<sup>1</sup>, 唐艳<sup>1</sup>

1. 四川大学 化学工程学院, 成都 610065; 2. 四川大学 材料科学与工程学院, 成都 610065

**摘要:** 分别采用固相-水热法和球磨法制备磷酸亚铁锂-磷酸钒锂复合正极材料 ( $\text{LiFePO}_4\text{-Li}_3\text{V}_2(\text{PO}_4)_3$ )。电化学性能测试表明,  $\text{LiFePO}_4\text{-Li}_3\text{V}_2(\text{PO}_4)_3$  复合正极材料的电化学性能远远高于  $\text{LiFePO}_4$  和  $\text{Li}_3\text{V}_2(\text{PO}_4)_3$  单独作为正极材料的性能, 并且以固相-水热法制备的复合材料性能优于以球磨法制得的复合材料。研究发现  $\text{LiFePO}_4\text{-Li}_3\text{V}_2(\text{PO}_4)_3$  复合材料有 4 个氧化还原峰, 相当于  $\text{LiFePO}_4$  和  $\text{Li}_3\text{V}_2(\text{PO}_4)_3$  氧化还原峰的叠加。采用固相-水热法制备的  $\text{LiFePO}_4\text{-Li}_3\text{V}_2(\text{PO}_4)_3$  复合材料形貌较为规则, 且有新相物质产生, 这是导致其电化学性能较好的原因。

**关键词:**  $\text{LiFePO}_4$ ;  $\text{Li}_3\text{V}_2(\text{PO}_4)_3$ ; 复合材料; 固相-水热法

(Edited by FANG Jing-hua)